

Oxygen Reduction Reaction at in Situ Fabricated Active Gold Over Layers in Acidic Media

Md. Rezwana Miah^{1,*}, Takeyoshi Okajima², Takeo Ohsaka^{3,*}

¹ Department of Chemistry, School of Physical Sciences, Shahjalal University of Science and Technology, Sylhet-3114, Bangladesh

² Department of Chemical Science and Engineering, School of Materials and Chemical Technology, Tokyo Institute of Technology, 4259-G1-5 Nagatsuta, Midori-ku, Yokohama 226-8502, Japan

³ Research Institute for Engineering, Kanagawa University, 3-27-1 Rokkakubashi, Kanagawa-ku, Yokohama 221-8686, Japan

*E-mail: mrmche@yahoo.com, pt120866sa@kanagawa-u.ac.jp

Received: 13 May 2016 / Accepted: 1 July 2016 / Published: 7 August 2016

Hydrous gold (Au) oxide, on polycrystalline Au (Au (poly)) electrode was *in situ* electrogenerated by multi-potential step amperometric (MPSA) technique between 2.2 V and 0.8 V with pulse time 0.001 s at each potential in 0.5 M H₂SO₄ solution for different times between 5-60 s. Electrodes with active gold over layers (agol) on the Au (poly) electrode (agol | Au (poly)) were generated by electroreduction of the hydrous Au oxide formed by MPSA technique. The agol | Au (poly) electrodes were characterized by reductive desorption of cysteine self-assembled monolayer (Cyst-SAM) and oxidative stripping of electrodeposited Pb. The *in situ* fabricated agol | Au (poly) electrode surface was found to be enriched in Au(100) and Au(110) domains as compared with the untreated Au (poly) electrode. Oxygen reduction reaction at the agol | Au (poly) electrode was carried out in 0.5 M H₂SO₄ solution. A significant catalysis of the ORR was achieved. The catalytic properties were explained in terms of crystalline domains and roughness factor of the Au electrode.

Keywords: Hydrous Au oxide; Active gold over layers; Roughness factor; Single crystalline domain; Oxygen reduction reaction

1. INTRODUCTION

It has been realized increasingly that many surfaces and interfacial processes of practical importance are affected significantly by the active metal over layers with rough surface morphology and preferential orientation of some crystalline domains. Smooth metal surface in terms of catalytic

and analytical properties for many electrochemical processes are significantly poor or inactive as compared with those of roughened or active metal over layer electrodes [1]. Metal over layers can be produced by the processes: (i) electrodeposition of highly dispersed metal nano-crystals on smooth substrates [2-7], (ii) from the vapor phase deposition of metals [8-12], (iii) chemical processes [13-14] and (iv) *in situ* formation of highly dispersed metal over layers from the electroreduction of hydrous metal oxide, formed by high potential anodization of the metallic electrodes [15-24].

Electrodes activated and roughened by the above-mentioned methods have very versatile applications towards many electrochemical processes. For example, the electrodes roughened by the electrodeposition of metal nano-crystals on smooth substrates play a key role in the determination of analytical and catalytic activities towards many electrochemical processes like oxygen reduction reaction (ORR) [2-4], oxidation of ethylene glycol [5], simultaneous determination of dopamine and ascorbate [6] and oxidation of glucose [7], etc. Vapor phase deposited metal thin films have been used for the ORR in acidic [8] and alkaline [9] media, oxidations of formaldehyde [10], acetaldehyde and ethanol [11]. Electrodes activated and roughened by chemical processes show a high catalytic effect towards the oxidation of methanol and other organic compounds [13-14]. Electrodes fabricated by anodization also have potential applications towards many electrochemical processes like oxidations of methanol [15, 18], carbon monoxide [18], ethanol [21], glucose [21, 22], ascorbic acid [21, 23] and heterocycle thiazole [24] and reduction of hydrogen peroxide [22], evolution of oxygen [19], etc.

Extensive studies have been done on *in situ* formation of the roughened active metal over layers, enriched in some single crystalline facets, by the electroreduction of hydrous metal oxides [25-33]. Such *in situ* produced porous metal over layers with high surface area have very complex topography consisting of metal clusters enriched in some single crystalline domains [8, 34-38]. L.D. Burke et al. studied hydrous Au oxide in terms of its formation [25], stability [26] and applications [27-31]. A.J. Arvia et al. conducted studies on columnar growth of hydrous Au oxide [32], ellipsometric experiments on the formation of hydrous Au oxide layers [33], STM-SEM and impedance studies on the characterization and mechanism of growth mode of hydrous Au oxide [39, 40], surface diffusion of Au atoms [41], change in the polycrystalline Au surface [42] and kinetics [43]. Juodkazis et al. [44, 45] carried out XPS and cyclic voltammetric studies on the hydrous Au oxide over layers for characterization and determination of surface Au atom concentration. Such electrodes having active metal over layers enriched in some preferential single crystalline domains with high surface area have supremacy over the electrodes obtained by either of the above processes from (i) to (iii) because of their wide applications, easiness of formation, stability, exclusion of the uses of extra chemicals and technical difficulties of the other processes.

In recent years, the ORR has become a subject of extensive studies because of its practical applications in fuel cells [46, 47], metal-air batteries [48], electrochemical caustic concentrators [49], air depolarized cathode [50] and oxidants production [51, 52], etc. To the best of our knowledge, application of electrogenerated active gold over layers of interest towards the ORR in any media has not been reported. Thus, in this paper, we report on the formation of active gold over layers on the Au (poly) electrode (agol | Au (poly)electrode) by electroreduction of hydrous Au oxide formed by MPSA technique in acidic media, its characterization using desorption of Cyst-SAM and stripping of electrodeposited Pb and its electrocatalytic activity towards the ORR in acidic aqueous media.

2. EXPERIMENTAL

For cyclic voltammetric measurements, Au (poly) electrodes with ($\phi = 1.6$ mm sealed in a Teflon jacket) an exposed surface area of 2.01×10^{-2} cm² were used as working electrode. A spiral Pt wire and an Ag / AgCl / NaCl (sat.) were the counter and reference electrodes, respectively. A conventional two-compartment Pyrex glass cell was used. Prior to each measurement either O₂ or N₂ gas was directly bubbled into the cell solution for 30 min to obtain O₂- or N₂-saturated solution and during measurements the gas was flushed over the cell solution. All the measurements were performed at temperature 25 ± 1 °C. The Au (poly) electrodes were polished with aqueous slurries of successively finer alumina powder (down to 0.06 μ m) and were sonicated for 10 min in Milli-Q water to remove the abrasive particles. The Au (poly) electrodes were then electrochemically pretreated in 0.5 M H₂SO₄ solution by repeating the potential scan in the range of -0.2 to 1.5 V vs. Ag / AgCl / NaCl (sat.) at 0.1 V s⁻¹ for 10 min or until the cyclic voltammetric characteristic of the clean Au electrode was obtained. Roughness factor was estimated by integrating the charge associated with the reduction of Au oxide using a cutting-weighing technique.

The agol | Au (poly) electrodes were fabricated as follows: Firstly, the hydrous Au oxide layers were grown on the Au (poly) electrode by applying MPSA between 2.2 and 0.8 V with pulse time 0.001 s at each potential for specified time ranging from 5 to 60 s in 0.5 M H₂SO₄ solution saturated under N₂ gas atmosphere. The lower potential such as 0.8 V was chosen in a such that any Au oxide formed with hydrous Au oxide undergoes reduction immediately and only hydrous Au oxide is accumulated on the surface. The preparation conditions were similar to previously reported articles [43, 53] in which the electrode was treated with square wave potential perturbation (SWPP) between 2.2 V and 0.8 V with a frequency of 1 kHz. After the MPSA treatment, the accumulated oxide was potential-stepped from 2.2 to 1.5 V for 1 min to sweep out any O₂ gas produced simultaneously with the hydrous Au oxide layer. Secondly, the hydrous Au oxide layers were electroreduced by applying a cathodic scan from 1.5 to -0.2 V and the agol | Au (poly) electrode thus fabricated was stabilized by a few more potential sweeps between -0.2 and 1.5 V prior to use.

The agol | Au (poly) electrode surface was characterized by cyclic voltammetric reductive desorption of Cyst-SAM and stripping of electrodeposited Pb. Cyst-SAM was fabricated by soaking the electrodes in 1.0 mM aqueous solution of cysteine for 10 min under open circuit potential. The electrodes were then thoroughly washed with Milli-Q water prior to electrochemical measurements for desorption of the Cyst-SAM. Pb was electrochemically deposited on the electrodes from an aqueous solution containing 1.0 mM Pb(NO₃)₂ using chronoamperometry. Electrochemical measurements were performed using an ALS 750B / HCH electrochemical analyzer.

3. RESULTS AND DISCUSSION

3.1 Formation of the agol / Au (poly) electrode in 0.5 M H₂SO₄ solution

Hydrous Au oxide on the Au (poly) electrode in 0.5 M H₂SO₄ solution was electrogenerated by MPSA technique under the conditions mentioned in Experimental section. The hydrous Au oxide

layers were subjected to electroreduction by applying linear sweep voltammetry (LSV) at scan rates ranging from 0.005 to 0.6 V s^{-1} . Fig. 1 (B) shows the corresponding typical LSVs obtained at scan rates of (c) 0.005 and (d) 0.1 V s^{-1} . A comparison of the curves (b) and (d) reveals that the electroreduction of hydrous Au oxide occurs at 0.35 V more negative potential as compared with that of the Au oxide.

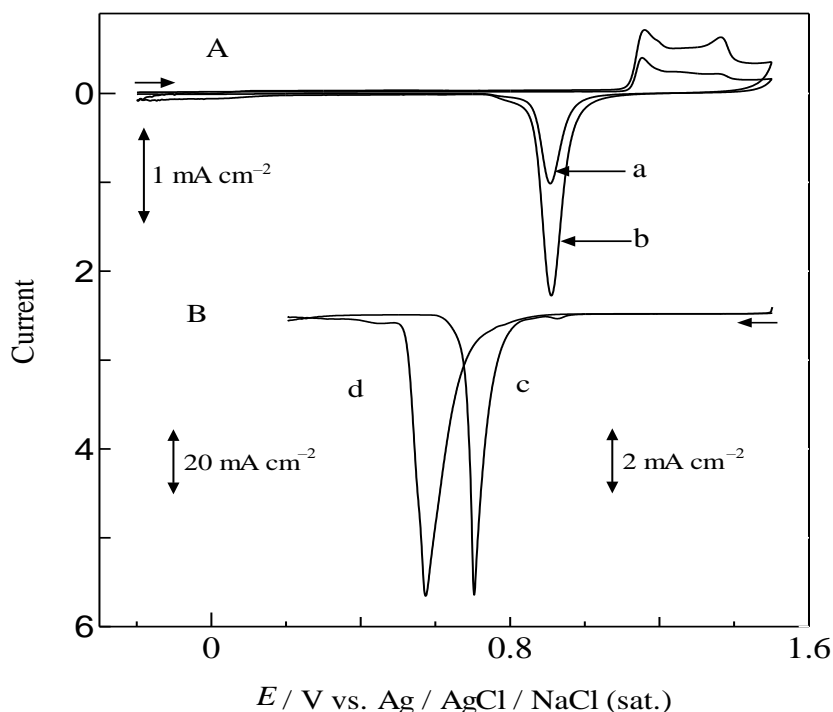


Figure 1. (A). CVs obtained in N_2 -saturated 0.5 M H_2SO_4 solution at a scan rate of 0.1 V s^{-1} using the (a) Au (poly) and (b) agol | Au (poly) electrodes. Time for the MPSA treatment of the agol | Au (poly) electrode was 10 s. (B) LSVs obtained in N_2 -saturated 0.5 M H_2SO_4 solution for the reduction of hydrous Au oxide at scan rates of (c) 0.005 and (d) 0.1 V s^{-1} . Treatment time for hydrous Au oxide generation was 20 s.

Furthermore the location of the peak position obtained for the reduction of hydrous Au oxide is strongly dependent on the scan rate. The peak potential is 0.7 V at scan rate of 0.005 V s^{-1} , while that at 0.1 V s^{-1} is 0.57 V. The charge associated with either peak (c) or (d) is largely greater than that of the peak (a) which was obtained for the untreated Au (poly) electrode indicating that the roughness of the agol | Au (poly) electrode was very high. The roughness factor (R) of the metal over layers strongly depends on the scan rate at which the hydrous Au oxide is reduced. Vela et al. [43] found that R increased from 1 to 50 only just by increasing the scan rate from 0.003 to 0.070 V s^{-1} and at higher scan rates the R remained ≈ 50 practically independent of the scan rate. For the electro-reduction at a fixed scan rate the R depends on the duration of the MPSA treatment for the formation of hydrous Au oxide. The R values of the agol | Au (poly) electrodes were obtained from the charge associated with the reduction of Au oxide derived by cutting-weighing technique. For the calculation of R , 0.420 mC charge was taken into account for the reduction of Au oxide formed on one square centimeter surface

[54] of the agol | Au (poly) electrodes. Fig. 2 shows the variation of R of the agol | Au (poly) electrodes with MPSA treatment time (t); the R increases from ca. 3.5 to 14.5 with increasing t from 5 to 60 s. The agol | Au (poly) electrodes used for the ORR were fabricated by the reduction of the hydrous Au oxide at a scan rate of 0.1 V s^{-1} .

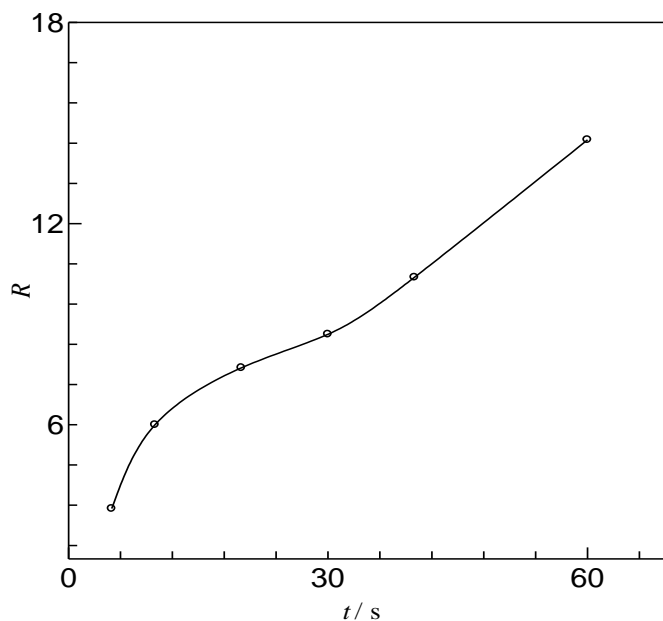


Figure 2. A plot of surface roughness factor (R) vs. MPSA treatment time (t). R was calculated by integrating the charge associated with the cathodic peak of LSVs (not shown) assigned to the reduction of Au oxide. The LSVs were recorded in N_2 -saturated $0.5 \text{ M H}_2\text{SO}_4$ solution at a scan rate of 0.1 V s^{-1} using the agol | Au (poly) electrodes obtained by MPSA treatment for 5–60 s.

3.2 Surface characterization of the agol /Au (poly) electrode using desorption of Cyst-SAM and Pb

The agol | Au (poly) electrodes exhibit a certain degree of preferred crystallographic orientations as it can be inferred from the change in the relative charge distribution of the anodic peaks located in the potential zone of 1.15–1.5 V in curve (b) in Fig. 1 (A). Reductive desorption of Cyst-SAM from the Au (poly) and agol | Au (poly) electrodes in N_2 -saturated 0.1 M KOH aqueous solution was used as a suitable technique for the determination of the relative ratios of different single crystalline domains of the agol | Au (poly) electrodes [23,55–58]. The values of ratio of charge consumed for the desorption of cysteine from the Au(100) and Au(110) facets to that of the Au(111) facet ($Q_{\text{Au}(100+110)}/Q_{\text{Au}(111)}$) were estimated by a cutting-weighting technique from CVs obtained for desorption of Cyst-SAM and are plotted against the MPSA treatment time (Fig. 3). This figure clearly shows that $Q_{\text{Au}(100+110)}/Q_{\text{Au}(111)}$ initially increases, passes through a maximum and then attains a level off trend at longer times. A maximum value of $Q_{\text{Au}(100+110)}/Q_{\text{Au}(111)}$ was obtained as 4.75 for MPSA treatment time of 10 s while the value was only 1.26 for the Au (poly) electrode. At longer treatment times than ca. 18 s the values of $Q_{\text{Au}(100+110)}/Q_{\text{Au}(111)}$ were found to be ca. 2.5 which are still higher than

that of the Au (poly) electrode. So, the interesting feature of the agol | Au (poly) electrodes is the enrichment of Au(100) and Au(110) facets on the surface unlike the untreated Au (poly) electrode.

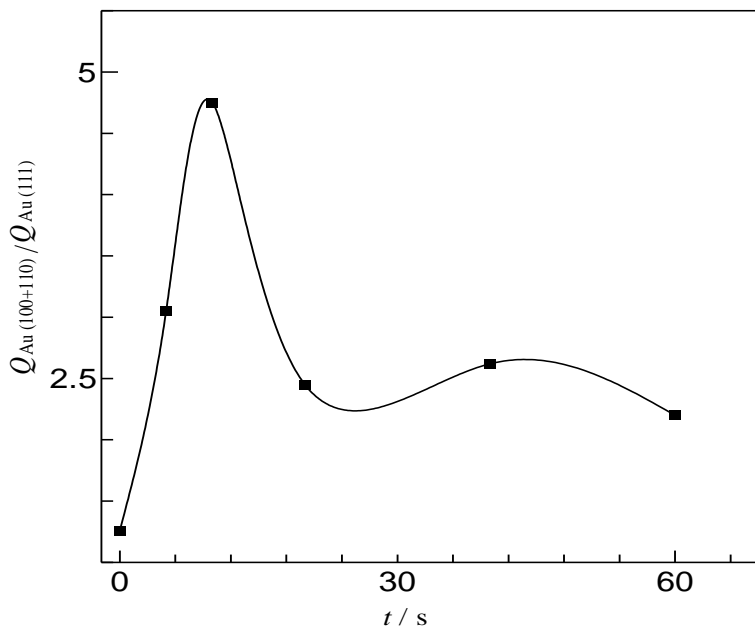


Figure 3. A plot of $Q_{\text{Au}(100+110)}/Q_{\text{Au}(111)}$ vs. MPSA treatment time (t) for the agol | Au (poly) electrodes. The values of $Q_{\text{Au}(100+110)}$ and $Q_{\text{Au}(111)}$ were calculated from CVs (not shown) obtained for the desorption of Cyst-SAMs in N_2 -saturated 0.1 M KOH solution in the potential range of 0.3 to -1.3 V at a scan rate of 0.1 V s^{-1} .

For further confirmation, oxidative stripping of electrodeposited Pb from the Au (poly) and agol | Au (poly) electrodes in N_2 -saturated 1.0 M HClO_4 solution at a scan rate of 0.1 V s^{-1} was also carried out [36, 37, 59, 60]. The stripping of Pb depends on the crystal phases, terrace length and step density of the electrode surface [60]. Pb was first deposited by amperometry by stepping the potential from 0 to -0.4 V for a deposition time of 5 s in 1.0 M HClO_4 solution containing 1.0 mM $\text{Pb}(\text{NO}_3)_2$ [59]. Fig. 4 shows the LSVs for the oxidative stripping of Pb from the (a) Au (poly) and (b) agol | Au (poly) electrodes. Two well defined peaks at 0.05 and -0.2 V and a shoulder peak at -0.17 V were observed for both of the Au (poly) and agol | Au (poly) electrodes. The sharp and the shoulder peaks at -0.2 and -0.17 V correspond to the stripping of Pb from the Au(111) facet and Au(111) terrace, respectively [60]. The relatively broader peaks located at 0.05 V correspond to the stripping of Pb from the Au(100) and Au(110) facets. The values of $Q_{\text{Au}(100+110)}/Q_{\text{Au}(111)}$ were 1.3 and 3.1 for the Au (poly) and agol | Au (poly) electrodes, respectively. The result is consistent with that obtained from the reductive desorption of the Cyst-SAMs. SWPP treatment condition-dependent variation in the ratio of crystalline facets of the active metal over layers was also reported by other researchers [34-38, 42].

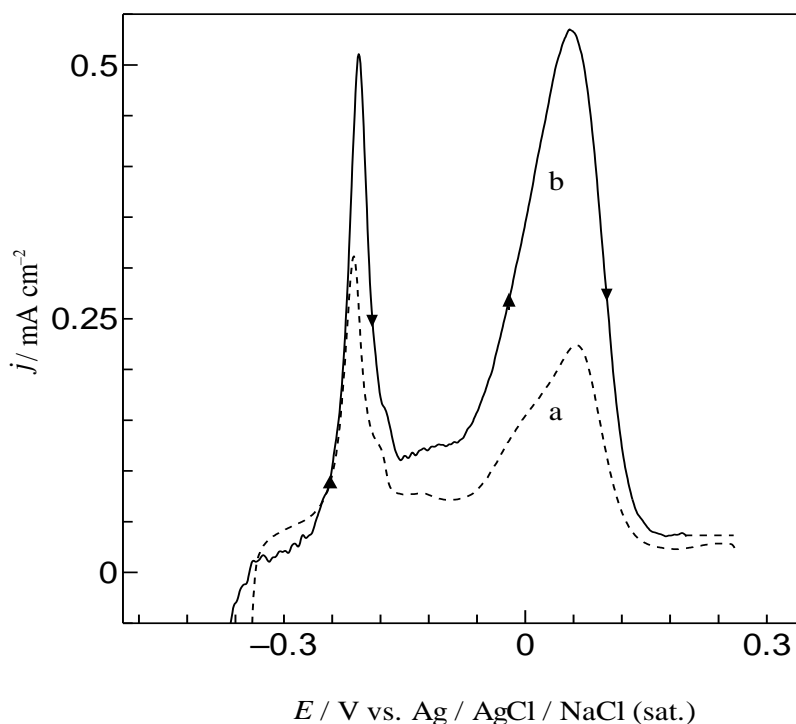


Figure 4. LSVs obtained for the oxidative stripping of Pb from the (a) Au (poly) and (b) agol | Au (poly) electrodes in N_2 -saturated 1.0 M $HClO_4$ + 1.0 mM $Pb(NO_3)_2$ solution at a scan rate of 0.1 V s^{-1} . The agol | Au (poly) electrode was obtained by MPSA treatment for 5 s.

3.3 ORR at the agol / Au (poly) electrode in 0.5 M H_2SO_4 solution

Fig. 5 shows the CVs obtained at the (a) Au (poly) and (b-c) agol | Au (poly) electrodes in O_2 -saturated 0.5 M H_2SO_4 solution containing (a-b) 0 and (c) 1 mM H_2O_2 at a scan rate of 0.1 V s^{-1} . The figure clearly shows two significant catalytic features obtained at the agol | Au (poly) electrode for the ORR. They are (i) a remarkable positive shift of the ORR potential and the splitting of the ORR peak at -0.2 V for the bare Au (poly) electrode into two peaks at $+0.05$ and -0.2 V and (ii) an increase in the peak current. At the Au (poly) electrode, the reduction peak at -0.2 V is due to the 2-electron reduction of O_2 to H_2O_2 and further reduction of H_2O_2 was not observed under the present experimental condition due to the overlapping with predominant evolution of H_2 . On the other hand, at the agol | Au (poly) electrode, two well-defined peaks at $+0.05$ and -0.2 V are observed for the 2-step 4-electron reduction of O_2 . The first reduction peak at $+0.05 \text{ V}$ is assigned to the reduction of O_2 to H_2O_2 presented by the reaction (1):



The second consecutive peak at -0.2 V is attributed to the further 2-electron reduction of H_2O_2 (2) which is produced by the reaction (1) as well as a direct 4-electron reduction of O_2 to H_2O (3).

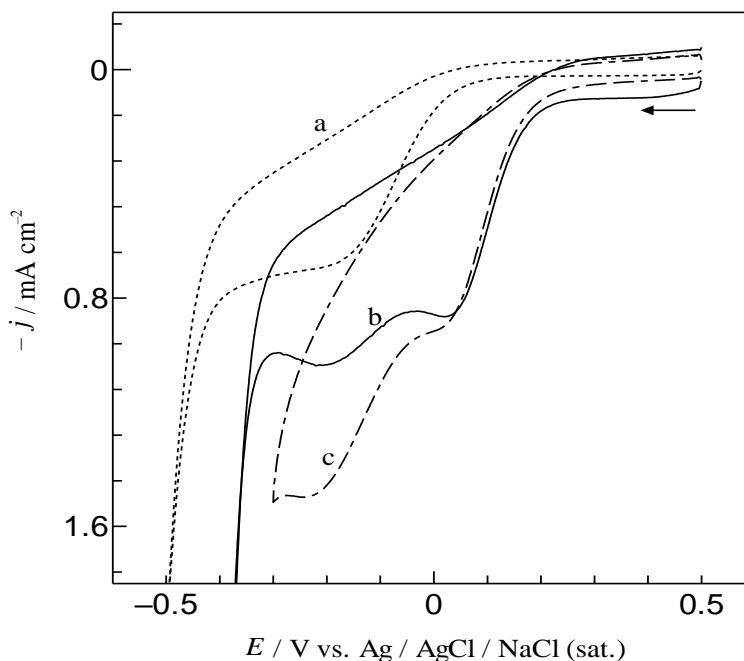


Figure 5. CVs obtained at the (a) Au (poly) and (b, c) agol | Au (poly) electrodes at a scan rate of 0.1 V s^{-1} in O_2 -saturated $0.5 \text{ M H}_2\text{SO}_4$ solution containing (a, b) 0 and (c) $1 \text{ mM H}_2\text{O}_2$. MPSA treatment time for the agol | Au (poly) electrode was 60 s .

The catalytic ability of the agol | Au (poly) electrode can be correlated to the (i) large surface area of the active gold over layers produced from the three-dimensional nucleation of Au atoms during the reduction of hydrous Au oxide and (ii) greater relative distribution of the Au(100) and Au(110) domains which are known to be more active towards the ORR than the Au(111) domains [61, 62]. Fig. 5 (c) shows the ORR at the agol | Au (poly) electrode in the presence of added $1 \text{ mM H}_2\text{O}_2$. The result shows that the peak current at $+0.05 \text{ V}$ remains unchanged while that at -0.2 V increases significantly due to the additional current from the reduction of the added H_2O_2 . Thus, it is confirmed that at potential around the peak current at -0.2 V , the reduction of H_2O_2 takes place nicely while the same reaction at the untreated Au (poly) electrode is very sluggish and requires high potential and overlaps with H_2 evolution. The agol | Au (poly) electrode, therefore, also has an enhanced catalytic activity towards H_2O_2 electroreduction. Owing to significant importance of detection of H_2O_2 in many biological and industrial cases, the catalytic reduction of H_2O_2 at the agol | Au (poly) electrode will be further explored elsewhere. The ORR at the agol | Au (poly) electrode was also carried out over a wide scan range of 0.01 to 1 V s^{-1} . Stable and reproducible responses were obtained corresponding to the 2-electron reduction of O_2 to H_2O_2 but the reduction peak at -0.2 V diminished at higher scan rates indicating a slow kinetic of H_2O_2 reduction. The plot of the first peak current (I_p^c) against the square root of scan rate was found to be almost linear (Fig. 6), indicating that the overall process is diffusion-

controlled. The first peak potential (E_{p1}^c) was plotted against $\ln(\nu / \text{V s}^{-1})$ and the result is shown in Fig. 7. The points fall on a straight line. The cathodic transfer coefficient (α_c) was calculated as 0.80 from the slope of the straight line [63]. The heterogeneous rate constant (k^0) was also estimated to be $2.3 \times 10^{-8} \text{ cm s}^{-1}$ from the intercept equal to 0.0167 V vs. Ag / AgCl / NaCl (sat) using the diffusion coefficient of O_2 ($1.93 \times 10^{-5} \text{ cm}^2 \text{ s}^{-1}$ [64]).

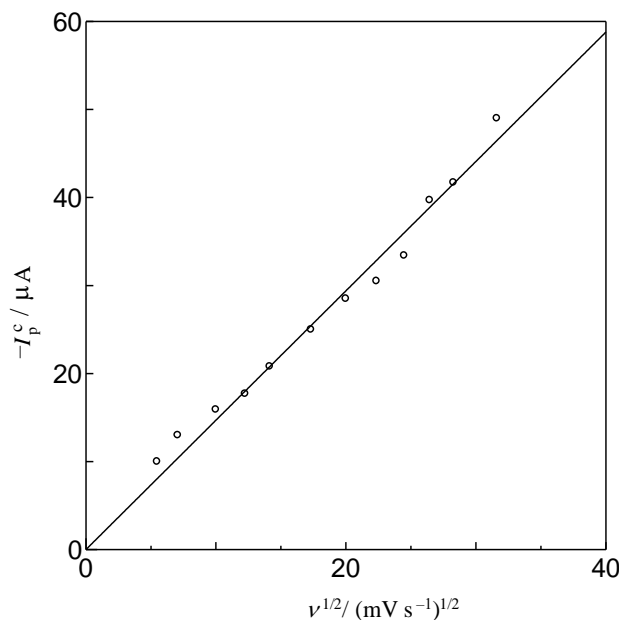


Figure 6. A plot of first peak current (I_p^c) vs. square root of scan rate ($\nu^{1/2}$) for the ORR at the agol | Au (poly) electrode. The peak currents were derived from CVs (not shown) obtained at the agol | Au (poly) electrode at different scan rates under the conditions mentioned in Fig. 5 (b).

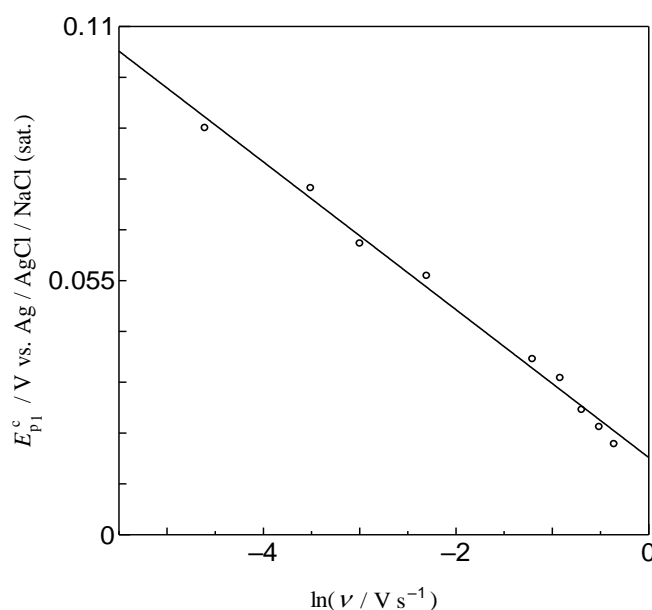


Figure 7. A plot of first peak potential (E_{p1}^c) vs. $\ln(\nu / \text{V s}^{-1})$ for the ORR at the agol | Au (poly) electrode. The peak potentials were derived from CVs (not shown) obtained at the agol | Au (poly) electrode at different scan rates under the conditions mentioned in Fig. 5 (b).

3.4. Effect of MPSA treatment time on the ORR at the agol /Au (poly) electrodes

Fig. 8 Shows the CVs obtained at the (a) Au (poly) and (b-e) agol | Au (poly) electrodes for the ORR in 0.5 M H₂SO₄ solution at a scan rate of 0.1V s⁻¹. MPSA treatment times (*t*) for the agol | Au (poly) electrodes were (b) 10, (c) 20, (d) 30 and (e) 60 s. The both peak potentials (E_{p1}^c and E_{p2}^c) for the ORR were found to shift to the more positive direction of potential with increasing *t*. From the comparison of the plot of E_{p1}^c vs. *t* (Fig.9) with Fig. 2, we can see that at *t* ≤ 30 s, both E_{p1}^c and *R* show a similar *t*-dependence but at longer *t*, E_{p1}^c shows a level off trend while *R* still increases. This result suggests that, at longer treatment times, more gold over layers are produced but they are deep seated and thus they do not have a significant role in enhancing the catalytic effect towards the ORR, probably due to the limitation of diffusion of O₂ into the pores of the deep seated layers. In addition, the longer treatment time reduces the relative distribution of the Au(100) and Au(110) domain to the Au(111) domain in which the former domains are more active for O₂ reduction than the latter one.

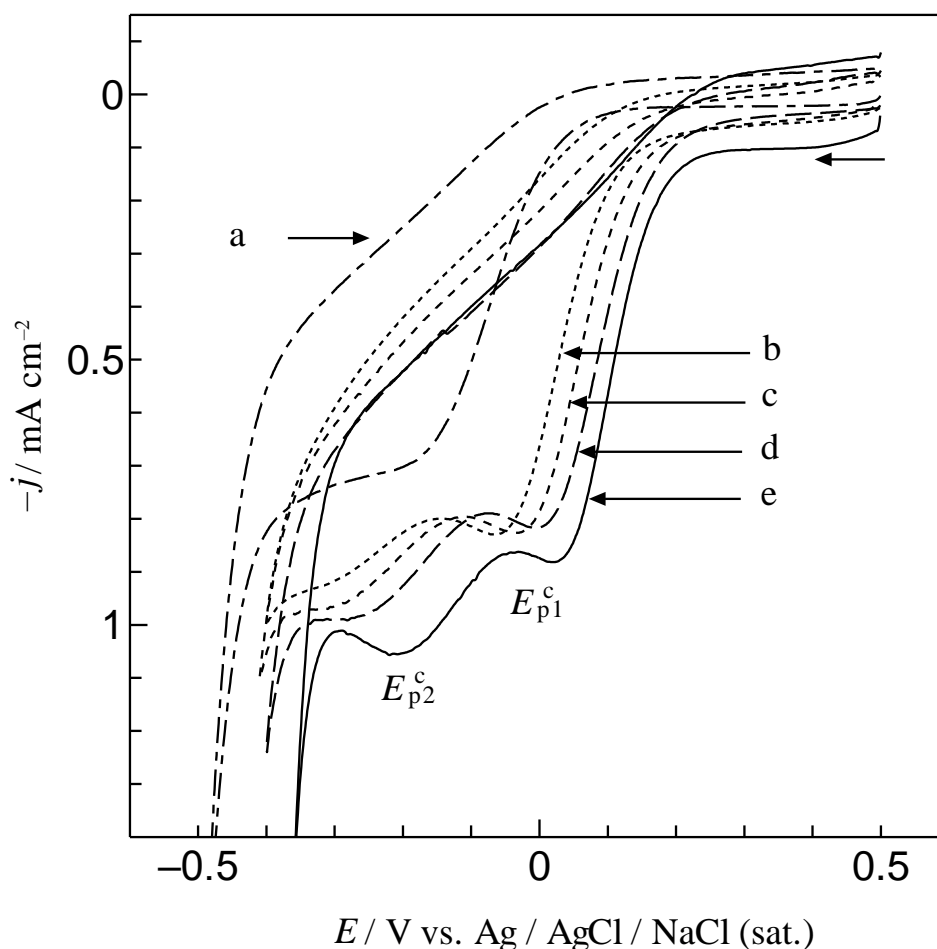


Figure 8. CVs obtained at the (a) Au (poly) and (b-e) agol | Au (poly) electrodes at a scan rate of 0.1 V s⁻¹ in O₂-saturated 0.5 M H₂SO₄ solution. MPSA treatment times for the agol | Au (poly) electrodes were (b) 10, (c) 20, (d) 30 and (e) 60 s.

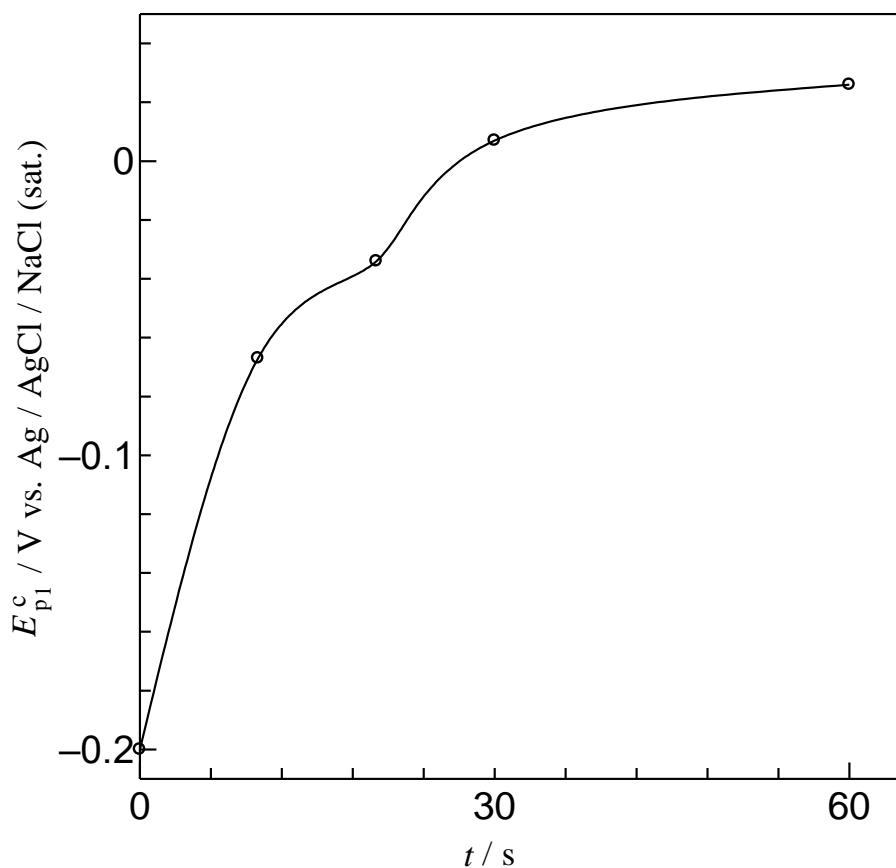


Figure 9. A plot of E_{p1}^c vs. MPSA treatment time (t). E_{p1}^c values were obtained from Fig. 8.

4. CONCLUSIONS

The agol|Au (poly) electrodes having active gold over layers were fabricated *in situ* by reduction of the hydrous Au oxide generated by MPSA treatment between 2.2 V and 0.8 V with pulse time 0.001 s at each potential in 0.5 M H₂SO₄ solution for 5-60 s. The relative distribution ratios of the Au(100) and Au(110) domain to the Au(111) domain of both of the Au (poly) and agol|Au (poly) electrodes were determined by reductive desorption of Cyst-SAM and stripping of electrodeposited Pb. The maximum value of $Q_{Au(100+110)}/Q_{Au(111)}$ for the agol|Au (poly) electrode was determined as ca. 5 while that for the Au (poly) electrode was only ca. 1.2. The roughness factor (R) varied in the range of 3.5-14.5 depending on the MPSA treatment time. The ORR was observed as two peaks. The first peak at +0.05 V was assigned to the 2-electron reduction of O₂ to H₂O₂ and the second one at -0.2 V was attributed to the further 2-electron reduction of H₂O₂ to H₂O. A 2-step 4-electron reduction of O₂ in acidic media was thus achieved at the agol|Au (poly) electrode, while at the Au (poly) electrode only a 2-electron reduction of O₂ to H₂O₂ takes place and further reduction of H₂O₂ was not observed actually possibly due to the overlapping with the significant evolution of H₂ gas. This electrode was also very active for H₂O₂ reduction. The catalytic activity was related to the higher ratio of the Au(100) and Au(110) domain to the Au(111) domain and the larger surface area compared with the untreated

Au (poly) electrode. Kinetics of the ORR at the agol|Au (poly) electrode and its electrocatalysis towards H₂O₂ reduction are currently examined and will be reported elsewhere.

ACKNOWLEDGEMENT

The present work was financially supported by Grant-in-Aid for Scientific Research from the Ministry of Education, Culture, Sports, Science and Technology (MEXT), Japan.

References

1. M. Haruta, *Catal. Today* 36 (1997) 153.
2. M.S. El- Deab and T. Ohsaka, *Electrochem. Commun.*, 4 (2000) 288.
3. M.S. El- Deab and T. Ohsaka, *Electrochim. Acta*, 47 (2002) 4255.
4. M.S. El- Deab and T. Ohsaka, *J. Electroanal. Chem.*, 553 (2003) 107.
5. A.A. El-Shafei, S.A. A. El-Maksoud and A.S. Fouda, *J. Electroanal. Chem.*, 395 (1995) 181.
6. C.R. Raj and T. Ohsaka, *J. Electroanal. Chem.*, 496 (2001) 44.
7. H. Jia, G. Chang, M. Lei, H. He, X. Liu, H. Shu, T. Xia, J. Su and Y. He, *Appl. Surf. Sci.*, 384 (2016) 58.
8. A. Sarapuu, K. Tammeveski, T. Toomas, Tenno, V. Sammelselg, K. Kontturi and D.J. Schiffrin, *Electrochem. Commun.*, 3 (2001) 446.
9. C. Paliteiro, A. Hamnett and J.B. Goodenough, *J. Electroanal. Chem.*, 234 (1987) 193.
10. K. Yahikozawa, K. Nishimura, M. Kumazawa, N. Tateishi, Y. Takasu, K. Yasuda and Y. Mastuda, *Electrochim. Acta*, 37 (1992) 453.
11. N. Tateishi, K. Nishimura, K. Yahikozawa, M. Nakagawa, M. Yamada and Y. Takasu, *J. Electroanal. Chem.*, 352 (1993) 243.
12. M. Mierzwa, W. Fabianowski, Ł. Górski, P. Smektała and T. Kobiela, *J. Electroanal Chem.*, 735 (2014) 63.
13. Z. Borkowska, A. Tymosiak-Zielinska, R. Nowakowski, *Electrochim. Acta*, 49 (2004) 2613.
14. R. Jurczakowski, C. Hirtz and A. Lasia, *J. Electroanal. Chem.*, 572(2004) 355.
15. M.K. Jeon and P.J. McGinn, *J. Power Sources*, 188 (2009) 427.
16. P. Iotov, S. Kalcheva and A.M. Bond, *J. Electroanal. Chem.*, 638 (2010) 275.
17. M. Jarosz, A. Pawlik, J. Kapusta-Kołodziej, M. Jaskuła and G.D. Sulka, *Electrochim. Acta*, 136 (2014) 412.
18. A. Velázquez-Palenzuela, E. Brillas, C. Arias, F. Centellas, J.A. Garrido, R.M. Rodríguez and P.-L. Cabot, *J. Power Sources* 208 (2012) 306.
19. M.E.G. Lyons, L. Russell, M. O'Brien, R.L. Doyle, I. Godwin and M.P Brandon, *Int. J. Electrochem. Sci.*,7(2012)2710.
20. M.P. Neupane, S. Park, S.J. Lee, K.A. Kim, M. H. Lee and T.S. Bae, *Int. J. Electrochem. Sci.*,4 (2009)197.
21. S. Xu, Y. Yao, P. Wang, Y. Yang, Y. Xia, J. Liu, Z. Li and W. Huang, *Int. J. Electrochem. Sci.*, 4 (2009) 197.
22. S. Xu, Y. Yao, Z. Li, H. Zhang, F. Huang and W. Huang, *Materials Lett.*, 82 (2012) 202.
23. J. Di, Y. Hu, Y. Song and Y. Tu, *J. Electroanal. Chem.*, 674 (2012) 12.
24. L.-H. Wang and K.-B. Jhang, *Electrochemistry*, 80 (2012) 968.
25. L.D. Burke and P.F. Nugent, *J. Electroanal. Chem.*, 444 (1998) 19.
26. L.D. Burke and J.F. O'Sullivan, *J. Electroanal. Chem.*, 285 (1990) 195.
27. L.D. Burke and J.F. O'Sullivan, *Electrochim. Acta*, 37 (1992) 2087.
28. L.D. Burke and J.K. Casey, *Electrochim. Acta*, 37 (1992) 1817.

29. L.D. Burke and B.H. Lee, *J. Electroanal. Chem.*, 330 (1992) 637.
30. L.D. Burke and T.G. Ryan, *Electrochim. Acta*, 37 (1992) 1363.
31. L.D. Burke and J.F. O'Sullivan, *Electrochim. Acta*, 37 (1992) 585.
32. M.E. Vela, S.L. Marchiano, R.C. Salvarezza and A.J. Arvia, *J. Electroanal. Chem.*, 388 (1995) 133.
33. M.E. Vela, J.O. Zerbino and A.J. Arvia, *Thin solid film*, 233 (1993) 82.
34. A.C. Chialvo, W.E. Triaca and A.J. Arvia, *J. Electroanal. Chem.*, 146 (1983) 93.
35. T. Izumi, I. Watanabe and Y. Yokoyama, *J. Electroanal. Chem.*, 303(1991) 151.
36. C.L. Perdriel, A.J. Arvia and M. Ipohorski, *J. Electroanal. Chem.*, 215 (1986) 317.
37. J. Gómez, L. Vázquez, A.M. Baró, C.L. Perdriel and A.J. Arvia, *Electrochim. Acta*, 34 (1989) 619.
38. A.J. Arvia, R.C. Salvarezza and W.E. Triaca, *Electrochim. Acta*, 34 (1989) 1057.
39. M.M. Gómez, L. Vázquez, R.C. Salvarezza, J.M. Vara and A.J. Arvia, *J. Electroanal. Chem.*, 317 (1991) 125.
40. L. Vazquez, A. Bartolome, A.M. Baro, C. Alonso, R.C. Salvarezza A.J. Arvia, *Surf. Sci.*, 215 (1989) 171.
41. C. Alonso, R.C. Salvarezza, J.M. Vara and A.J. Arvia, *Electrochim. Acta*, 35 (1990) 1331.
42. A.C. Chialvo, W.E. Triaca and A.J. Arvia, *J. Electroanal. Chem.*, 171 (1984) 303.
43. M.E. Vela, R.C. Salvarezza, and A.J. Arvia, *Electrochim. Acta*, 35 (1990) 117.
44. K. Juodkazis, J. Juodkazyte, V. Jasulaitiene, A. Lukinskas and B. Sebek, *Electrochem. Commun.*, 2 (2000) 503.
45. K. Juodkazis, J. Juodkazyte, B. Sebek and A. Lukinskas, *Electrochem. Commun.*, 1 (1999) 353.
46. G. Guillaume, E. David, F. Katia and G. Pierre, *J. Solid State Electrochem.*, 20 (2016) 1539.
47. D. Yu-Jia, T. Vladimir, R. Jan and A. Matthias, *ACS Catal.*, 6 (2016) 671.
48. C.C Wang, K.S. Goto and S.A. Akbar, *J. Electrochem. Soc.*, 138 (1991) 3673.
49. N.R.K. Vilambi and E.J. Taylor, *Sep. Sci. Technology*, 25 (1990) 627.
50. M. Sudoh, T. Koder, H. Hino and H. Shimamura, *J. Chem. Eng. Jpn.*, 21 (1998) 198.
51. J.J. Jow, A.C. Lee and T.C. Chou, *J. Appl. Electrochem.*, 17 (1987) 753.
52. C. Olman and A.P. Watkinson, *J. Appl. Electrochem.*, 9 (1979) 117.
53. A.C. Chialvo, W.E. Triaca and A.J. Arvia, *J. Electroanal. Chem.*, 171 (1984) 303.
54. P.S. Germain, W.G. Pell and B.E. Conway, *Electrochim. Acta*, 49 (2004) 1775 and references therein.
55. M.S. El-Deab and T. Ohsaka, *Electrochem. Commun.*, 5 (2003) 214.
56. W. Yang, J.J. Gooding and D. Brynn Hibbert, *J. Electroanal. Chem.*, 516 (2001) 10.
57. C.A. Widrig, C. Chung and M.D. Porter, *J. Electroanal. Chem.*, 310 (1991) 335.
58. D. Zhang, L. Mao, J. Wu, T. Okajima, F. Kitamura and T. Ohsaka, *Jpn. J. Deuterium Sci.*, 11 (2002) 557.
59. M.O. Finot, G.D. Braybrook and M.T. McDermott, *J. Electroanal. Chem.*, 466 (1999) 234.
60. M.M. Walczak, C.A. Alves, B.D. Lamp and Marc D. Porter, *J. Electroanal. Chem.*, 396 (1995) 103.
61. S. Strbac and R.R. Adzic, *J. Electroanal. Chem.*, 403 (1999) 169.
62. R.R. Adzic, N.M. Markovic and V.B. Vesovic, *J. Electroanal. Chem.*, 165 (1984) 105.
63. A.J. Bard and L.R. Faulkner, *Electrochemical Methods-Fundamentals and Applications*, John Wiley & Sons, Inc., Chapter 6 (1980).
64. Md. R. Miah and T. Ohsaka, *Electrochim. Acta*. 54 (2009) 5871.